International Journal of Thermal Sciences 199 (2024) 108933

Contents lists available at ScienceDirect

International Journal of Thermal Sciences

journal homepage: www.elsevier.com/locate/ijts

Thermal characterisation of the cooling phase of post-flashover compartment fires

Andrea Lucherini [a,b,*], Balša Jovanović [b], Jose L. Torero [c], Ruben Van Coile [b], Bart Merci [b]

[a] Department for Research of Fire-Safe Sustainable Environment (FRISSBE), Slovenian National Building and Civil Engineering Institute (ZAG), Slovenia
[b] Department of Structural Engineering and Building Materials, Ghent University, Belgium
[c] Department of Civil, Environmental & Geomatic Engineering, University College London, UK

ARTICLE INFO

Keywords:
Cooling phase
Fire decay
Fire dynamics
Compartment fires
Structural fire engineering
Fire safety

ABSTRACT

The main characteristics of the cooling phase of post-flashover compartment fires are studied using a simplified first-principles heat transfer approach to establish key limitations of more traditional methodologies (e.g., Eurocode). To this purpose, the boundary conditions during cooling are analysed. To illustrate the importance of a first-principles approach, a detailed review of the literature is presented followed by the presentation of a simplified numerical model. The model is constructed to calculate first-order thermal conditions during the cooling phase. The model is not intended to provide a precise calculation method but rather baseline estimates that incorporate all key thermal inputs and outputs. First, the thermal boundary conditions in the heating phase are approximated with a single (gas) temperature and the Eurocode parametric fire curves, to provide a consistent initial condition for the cooling phase and to be able to compare the traditional approach to the first-principles approach. After fuel burnout, the compartment gases become optically thin and temperatures decay to ambient values, while the compartment solid elements slowly cool down. For simplicity, convective cooling of the compartment linings is estimated using a constant convective heat transfer coefficient and all linings surfaces are assumed to have the same temperature (no net radiative heat exchange). All structural elements are assumed to be thermally thick. While these simplifications introduce quantitative errors, they enable an analytical solution for transient heat conduction in a semi-infinite solid that captures all key heat transfer processes. Comparisons between the results obtained using both approaches highlight how, even when considering the same fire energy input, the thermal boundary conditions according to the Eurocode parametric fire curves lead to an increase energy accumulated in the solid after fuel burnout and a delay in the onset of cooling. This is not physically correct, and it may lead to misrepresentation of the impact of post-flashover fires on structural behaviour.

1. Introduction and background

Ensuring the structural stability and integrity of a building in case of fire is of the utmost importance for the safety of its occupants and firefighters as well as for other fire safety objectives, such as property protection and business continuity. Traditional prescriptive design methodologies for structural systems exposed to fire are based on the concept of the standard fire curve as the main design scenario for post-flashover compartment fires [1]. This fire exposure is characterised by a monotonically increasing temperature-time curve, deemed to represent a worst-case scenario for non-combustible construction materials during the growth and fully-developed phases of a fire [2,3]. However, the past two decades of research have highlighted the need to adopt a holistic performance-based methodology for the design of structures that ensures structural integrity and stability. Thus, it is necessary to deliver a performance analysis of the structure using a more realistic thermal exposure until complete fuel burnout [4]. This approach allows then to analyse the structural behaviour of load-bearing systems during all phases of a fire: growth, fully-developed, decay, and cooling.

Given that structural design seeks to optimize materials usage, the literature highlights the importance of understanding the behaviour of the structure during the fire decay and cooling phase. Once the fuel has been consumed, the structure continues to evolve thermally and, given common structural optimization practises, thermal evolution after the heating phase can lead to failure. Therefore, the cooling of the structural

* Corresponding author. Department for Fire-Safe Sustainable Built Environment (FRISSBE), Slovenian National Building and Civil Engineering Institute (ZAG), Dimiceva ulica 12, 1000 Ljubljana, Slovenia
E-mail address: andrea.lucherini@zag.si (A. Lucherini).

https://doi.org/10.1016/j.ijthermalsci.2024.108933
Received 14 April 2023; Received in revised form 16 January 2024; Accepted 23 January 2024
Available online 2 February 2024

Nomenclature

T	Temperature [K]
ΔT	Temperature difference [K]
T_s	Surface temperature [K]
T_g	Compartment gases temperature [K]
$T_{s,max}$	Maximum surface temperature [K]
T_w	Compartment linings surface temperature [K]
T_a	Ambient temperature [K]
T_i	Initial temperature [K]
T_{SFC}	Temperature from standard fire curve [K]
T_{EPFC}	Temperature from Eurocode parametric fire curve [K]
L_k	Characteristic length [m]
H	Compartment height [m]
H_o	Compartment opening height [m]
t_k	Characteristic time [s]
t_{max}	Heating period duration [s]
L_{th}	Thermal penetration depth [m]
A_o	Compartment opening surface [m^2]
A_W	Compartment linings surface [m^2]
A_t	Total compartment surface [m^2]
h_c	Convective heat transfer coefficient [W/m^2K]
O	Opening factor [$m^{0.5}$]
b	Thermal inertia [$J/m^2s^{0.5}K$]
λ	Thermal conductivity [W/mK]
α	Thermal diffusivity [m^2/s]
ρ	Density [kg/m^3]
c_p	Specific heat capacity [J/kgK]
d	Thickness [m]
ε	Emissivity [−]
F_{ij}	View factor [−]
σ	Stefan–Boltzmann constant [5.67×10^{-8} W/m^2K^4]
q''_f	Fuel load density [MJ/m^2]
dQ_{CV}/dt	Rate of energy change within the control volume [W]
$\dot{Q}_{fire}$	Fire heat release rate [W]
$\dot{Q}_{flow,in}$	Convective heat entering the control volume per unit time [W]
$\dot{Q}_{flow,out}$	Convective heat leaving the control volume per unit time [W]
$\dot{Q}_{wall}$	Conductive heat to the enclosure boundaries per unit time [W]
$\dot{Q}_{rad}$	Radiative heat through the opening per unit time [W]
$\dot{m}_a$	Mass flow rate of air at opening [kg/s]
$\dot{m}_g$	Mass flow rate of compartment gases at opening [kg/s]
$\dot{m}''_f$	Fuel burning rate [kg/s]
ΔH_c	Fuel heat of combustion [J/kg]
$\dot{q}''_{conv}$	Convective heat flux [W/m^2]
$\dot{q}''_{rad}$	Radiative heat flux [W/m^2]
$\dot{q}''_{net}$	Net heat flux [W/m^2]
$\dot{q}''_{cond}$	Conduction heat flux [W/m^2]
E''_{th}	Thermal energy per unit area [J/m^2]
t	Time [s]
x	Space, depth [m]
g	Gravitational acceleration [9.81 m/s^2]
n	Multiplication factor [−]

systems is relevant, independently of the construction materials used.

With regards to concrete structures, during a fire, the temperatures inside concrete members continue to evolve after the period of maximum gas temperature. This means that the highest temperatures in the reinforcement might occur during the fire decay or cooling phase [5]. Furthermore, concrete can experience an overall further loss of strength while cooling [6,7]. These effects depend on many variables, including heating rates. Studies have shown that the effects of the fire on the structure are potentially more critical for fast-growing fires (steep temperature gradients) than for slowly growing ones [8], thus similar differences could be expected for fast or slow cooling. It is also expected that these consequences may be more critical for structural elements with 3- or 4-side fire exposure (i.e., beams and columns) [9–11].

Steel structures typically experience large variations in the force distributions within a structural frame during a fire event [12]. During the heating phase, steel connections usually suffer large forces due to thermal expansions and deformations of longitudinal elements, while during cooling high tensile stresses challenge steel connections due to the thermal contraction of the same longitudinal elements [13]. The specific characteristics of the cooling phase can therefore impact the behaviour of a steel structure in this latter stages of a fire event.

Finally, the fire decay and cooling phases can also challenge wooden structural systems because, when the contents-fire extinguish, the heat wave continues to propagate within the timber and, accordingly, the load-bearing capacity of the structural system can, potentially, continue to decrease [14–19]. The problem is more critical for timber structures because wood irreversibly loses its mechanical properties at relatively low temperatures, compared to traditional construction materials like steel and concrete. For example, at 100 °C a typical softwood column has a reduction of compressive capacity of about 75 %, compared to its capacity at ambient temperature [20], and the zero-strength layer within timber cross-sections can extend to areas at temperatures as low as 90 °C [19,21]. A problem, specific to timber, is the influence of internal temperature gradients on self-extinction [22]. Conditions during fire decay and cooling can delay self-extinction enhancing the potential for challenging behaviour such as delamination.

Consequently, for all construction materials, structural failure can occur during the fire decay and subsequent cooling, even hours after a fire is extinguished [10]. The main challenge is related to the fact that, after fire extinction, this hazard cannot be easily detected, and structural collapse may occur with little or no warning. This situation is a critical scenario for fire brigade interventions. This is what happened in Switzerland in 2004, when an underground car park collapsed after fire extinguishment, claiming the lives of seven firefighters [23].

Historically, most of the research efforts have been directed towards comprehending the thermal effects of a fully-developed fire during heating, which leads to the highest heat fluxes and temperatures, and it is commonly considered as the most challenging phase for load-bearing systems. It is also common to find large-scale compartment fire test results where the fire decay and cooling phases are not even characterised/reported. Due to safety concerns, in many cases, the fire is manually extinguished with water rapidly cooling all structural systems [24]. As a result, engineering tools, aimed at estimating the thermal conditions to load-bearing systems in the event of a fire, focus on the maximum temperature achieved by the structure during the fully-developed phase of the fire, and little interest has been devoted to the fire decay and cooling phases [25,26].

Given the recognition that structural behaviour in fire needs to be optimized and explicitly assessed, burnout needs to be characterised, therefore various models that also include the fire decay and cooling phases have been developed and included in structural fire engineering design practices [27]. Existing computer models solve the conservation equations to estimate the fire conditions in post-flashover compartments and have the capacity to introduce burnout and the subsequent cooling phase [27]: from simplified single- or two-zone models (e.g., OZone [28,29], CFAST [30], and B-RISK [31]) to higher complexity computational

fluid dynamics (CFD) software [32] (e.g., Fire Dynamics Simulator - FDS [33]). These models are in some cases coupled with a finite-element model for structural analysis (e.g., SAFIR [34] and OpenSEES [35]). Despite their physical basis, all these models impose strong simplifications and approximations while remaining of complex use. Many of these approximations and simplifications reside within inputs and are many times hidden under the complexity of the modelling strategy. Simpler approaches seem to remain necessary and are currently used widely for design purposes.

The most widely adopted methodology to characterise natural fire conditions for structures is a heat transfer analysis that uses as input the temperature histories provided by the Eurocode parametric fire curves (EPFC) [36], which were developed starting from the Swedish fire curves [37–40]. This method offers analytical expressions to generate the temperature-time history of a fire as a function of the fuel load density and the ventilation factor as first described by Thomas [25]. The thermo-physical properties of linings materials also form part of the definition of these curves. However, in its current formulation, the cooling phase is substantially simplified into a linear decay relationship, following constant cooling rates as prescribed in the 1975 edition of the ISO 834 standard, which are not based on fundamental physical principles or a comprehensive research study [38,41]. This approach can lead to a potentially unrealistic definition of the cooling phase [42,43], nevertheless there is no detailed quantitative or qualitative evaluation of the nature or magnitude of potential errors introduced through this simplification.

Over the past decades, several other engineering approaches to estimate the thermal conditions of natural fires on structural elements have also been proposed. These methodologies rely on different assumptions and simplifications. Examples are the formulations given by the BFD temperature-time curves, obtained by Barnett through an empirical regression analysis of full-scale experiments [44–46] and the iBMB parametric fire curves, implemented in the German national annex of EN 1991-1-2. In the latter case, the heating curves offer a method similar to the Eurocode parametric fire curves, but the cooling phase is defined as a parabolic decay curve [47,48]. No substantial evidence for the choice of mathematical representation is provided. Other methods of various complexities and based on different sets of experimental data can be also found in other studies [49–52]. A comparison of different approaches is shown in Fig. 1. Fig. 1 offers an example of the several temperature-time curves that can be obtained for a specific post-flashover compartment fire, and it compares the modelled temperature histories to those obtained experimentally from a large-scale fire test [53]. All the graphs have been shifted to have the same flashover time, defined at a smoke layer temperature above 550 °C [54]. While Fig. 1 seems to demonstrate agreement between models and experiments, this is purely based on temperature measurements and does not describe the heat transfer environment. Furthermore, the lack of detail on the radiative heat exchange corrections for the thermocouples makes it difficult to assess where the temperatures can be used as input for heat transfer calculations. This was made evident by Welch et al. [55] who showed the importance of these corrections when the gas was optically thin.

Overlooking or highly simplifying the fire decay and cooling phases can affect the accuracy of any heat transfer calculations to the structure and therefore, potentially hiding dangerous failure modes. Comprehending and properly considering the fire decay and cooling phases can therefore significantly improve performance-based design methodologies that aim to deliver fire-safe structures. This study aims to provide an assessment of the different factors influencing the thermal boundary conditions for a structure in the event of a fire. The focus is on the decay and cooling phases. This study does not aim at producing a precise method of assessment, instead it attempts to analyse the problem with simple tools that are based on fundamental principles, enabling a transparent discussion of assumptions and limitations. Thus, the current research study describes the principles and characteristics of natural fires in post-flashover compartments, considering both the heating phase and the cooling phase. Based on energy conservation equations, a simplified numerical model is introduced to approximate the thermal conditions to structural elements within an enclosure during the cooling phase and define appropriate thermal boundary conditions. Simplifications and assumptions are discussed in detail enabling a clear understanding of the potential impact of each simplification and assumption on the thermal evolution of the structure. The presented methodology aims at highlighting the importance of approaching the problem of the cooling phase from a first-principles perspective, suggesting the use of analytical solutions and various simplifications to properly treat the convective and radiative heat transfer.

2. Phases of post-flahover compartment fires

A natural fire within a building enclosure is typically composed of a growth, a fully-developed, a decay, and a cooling phase [54,56]. After fire ignition, the *growth phase* is characterised by a gradual increment of

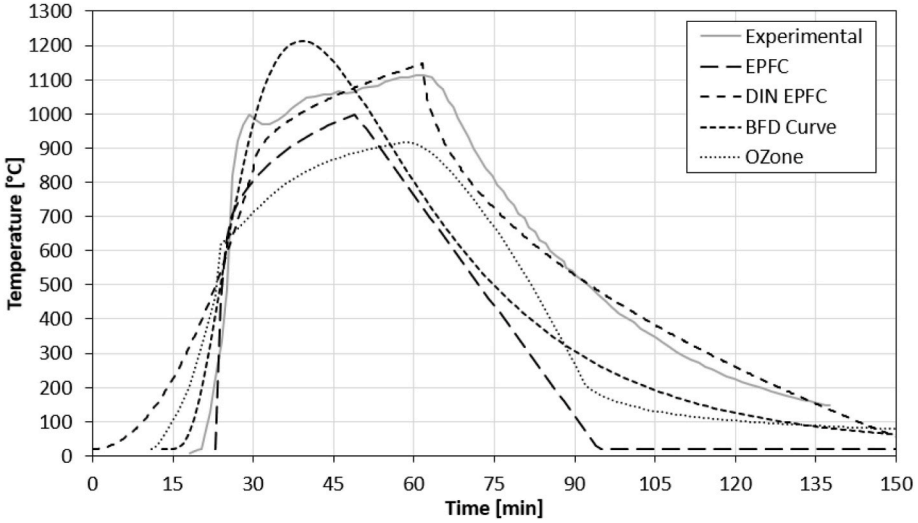

Fig. 1. Comparison between experimental results (Test 8, Cardington fire tests [53]) and various methodologies to estimate temperature-time curve of post-flashover compartment fires. For purposes of illustration, the curves were shifted to achieve flashover at the same instant. While it is recognised that flashover is a complex process, the instant where flashover occurs is defined as when the temperature reaches 550 °C [54].

the fire heat release rate, and the average compartment temperature and heat fluxes are relatively low, as the fire is localised in the vicinity of its origin. If the conditions are met, at flashover all combustible items in the compartment ignite simultaneously and flames appear to fill essentially the entire volume. There is a rapid increase in the fire heat release rate and compartment temperature. Depending on the compartment and fuel characteristics, the *fully-developed phase* of the fire can be typically associated with a quasi-constant heat release rate (ventilation- or fuel-controlled) and homogeneous temperature.

Regarding the stability and integrity of load-bearing elements, structural fire engineering usually focuses on post-flashover fires because, after flashover, the thermal attack caused by the fire is significant. Consequently, the mechanical strength and stiffness of construction materials and structural systems can be significantly affected, and the stability and integrity of load-bearing elements can be compromised [57]. The pre-flashover and the fully-developed phase traditionally represent the heating phase of the structure during a fire event. After that, the fire starts decreasing, leading to the fire decay and cooling phases.

The fire decay phase and the cooling phase are often mixed up in the literature. However, they refer to two slightly different periods of the fire. This distinction has been recently underlined and associated with the time-history of fire heat release rate [56].

Within the *fire decay phase,* there is still a "fire", therefore during this phase there is still some flaming combustion taking place in the compartment, hence the fire heat release rate is different from zero. The decay phase is characterised by a progressive transformation of the fire from a fully-developed fire, where heat generation from the fire is a critical term in the energy equation, to a fire where heat generation can be neglected and eventually disappears from the energy equation. In this phase, structural elements can still heat up as long as they receive a positive heat flux, therefore the fire decay phase can still be part of the heating phase for the structure [36,56].

On the other hand, in the *cooling phase*, the fire is extinguished and therefore there is no heat release. After burnout, the total amount of energy within the compartment control volume decreases (i.e. the compartment gases and solids are losing heat to the surrounding environment). Nevertheless, the compartment elements still exchange heat between them. Structural elements, as any other component within the compartment, cool down according to their material properties and the conditions in the surrounding environment (e.g., compartment gases and linings). This phenomenon primarily depends on the characteristics of the compartment (e.g., geometry and opening) and its elements (e.g. linings).

In some models available in the literature, the fire decay phase is assumed to start when 70–80 % of the total fuel load has been consumed and, after this point, the fire heat release rate decreases linearly to zero [28,29,36,41,58]. However, there is no conclusive data on the amount of heat being released in the decay phase. The transition is highly fuel-dependent, and the available literature offers little evidence on the decay period of the heat release rate of post-flashover compartment fires [56].

Therefore, as in other simplified models (e.g., Eurocode parametric fire curves, discussed in section 7.1), this study assumes that the end of the fire fully-developed phase corresponds to complete fuel burnout [56]. Hence, all the fuel is assumed to fully combust during the fully-developed phase, the fire heat release rate instantaneously drops to zero, and no fire decay phase is considered. From a structural point of view, this is generally considered to represent a more critical case for traditional load-bearing elements because it leads to a longer fully-developed phase and, therefore a higher maximum temperature and longer exposure to higher temperatures. For consistency with future work, this research study exclusively refers to the cooling phase as the phase after the fully-developed phase (without a fire decay phase).

3. Compartment energy balance

In a fire event, the gas phase enclosed by the compartment can be considered as a control volume of constant volume. While making the control volume the size of the compartment represents a very strong simplification that eliminates all terms associated with the distribution and transfer of energy within the compartment, the detail of Equation (1) is sufficient for the purposes of this study. As illustrated in Fig. 2, the energy conservation equation for the compartment enclosure is usually described as follows [57,59]:

$$\frac{dQ_{CV}}{dt} = \dot{Q}_{fire} + \left(\dot{Q}_{flow,in} - \dot{Q}_{flow,out}\right) - \dot{Q}_{wall} - \dot{Q}_{rad} \tag{1}$$

where dQ_{CV}/dt [W] is the rate of energy change within the control volume, $\dot{Q}_{fire}$ [W] is the total heat release rate (HRR) within the enclosure by the fire, $\dot{Q}_{flow,in}$ and $\dot{Q}_{flow,out}$ [W] are the energy entering and leaving the control volume per unit time by flows through the opening, $\dot{Q}_{wall}$ [W] represents the rate of heat transferred to (+) or from (−) the enclosure boundaries (load-bearing or not), and $\dot{Q}_{rad}$ [W] represents the radiative heat per unit time transferred through the opening.

The described terms play different roles in the energy balance within the compartment. Their order of magnitude is very diverse, and their signs can vary depending on the heat gains or heat losses. For the purposes of this study and simplification, the opening is assumed much smaller than the surface area of the inner boundaries and, accordingly, the radiative heat transfer from the hot gases through the opening ($\dot{Q}_{rad}$) can be assumed to be negligible (less than 10 % for the presented case). Furthermore, while radiation losses through the openings might not be negligible (large openings, optically thick gas phase, etc.), for small openings, and when integrated over the duration of the fire, it has been estimated to be approximately 3 % of the total energy released [58]. Thus, the assumption is limited but not incorrect, and given that the heating of the compartment elements is the result of a process of heat transfer integrated over time, it is reasonable to neglect this term.

3.1. Heating phase

The fire growth phase and in particular the fire fully-developed phase are usually considered the main heating phases for load-bearing structural systems. As shown in Fig. 3, the energy contribution of the fire heat release rate ($\dot{Q}_{fire}$) and the heat exchange at the compartment opening ($\dot{Q}_{flow}$) and linings ($\dot{Q}_{wall}$) define the compartment fire dynamics, and they must be analysed and quantified in detail. Accordingly, Equation (1) during the heating phase can be re-written as follows:

$$\frac{dQ_{CV}}{dt} = \dot{Q}_{fire} + \dot{Q}_{flow,in} - \dot{Q}_{flow,out} - \dot{Q}_{wall} \tag{2}$$

By adopting simplifying assumptions, the various terms can be estimated, and the differential equation can be solved. A classic simplification formulates that heat release rate by the fire and advective heat

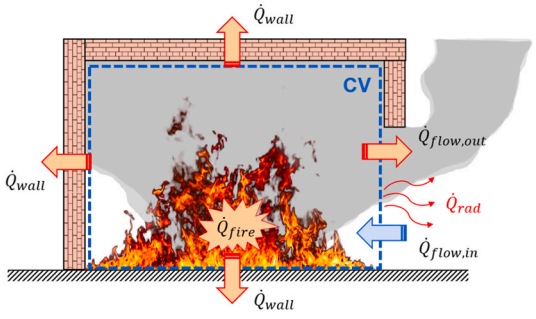

Fig. 2. Energy balance within the fire compartment (control volume, CV).

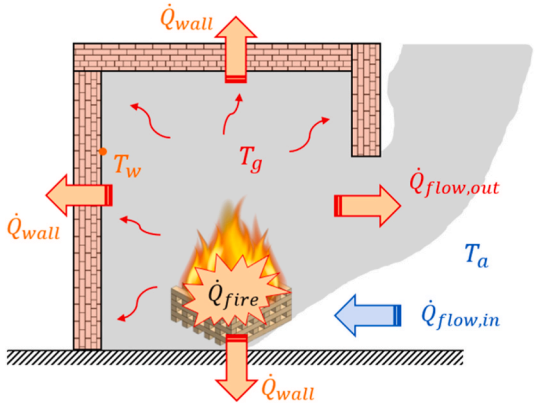

Fig. 3. Side view schematisation of heating phase.

transfer flowing outwards through openings ($\dot{Q}_{flow,out}$) dominate the fire dynamics within a compartment, with $\dot{Q}_{flow,in}$ can generally considered negligible (compared to $\dot{Q}_{flow,out}$) [60]. These assumptions and the additional simplification of a homogeneous control volume allow for the thermal conditions to compartment elements during the heating phase to be defined by a single temperature evolving in time. Thomas [61] suggests that the maximum gas phase temperature (attained at steady state) is the conservative compartment temperature that should be used to quantify heat transfer to the compartment elements. This approach is typically valid for relatively small compartments, but the assumption of homogenous temperature distribution is no longer valid for large compartments, particularly if the aspect ratio deviates from cubic compartments. Many examples of non-homogeneous compartment temperatures have been reported and reviewed by Stern-Gotfried et al. [62]. A more recent example has been reported by Gupta et al. [63] who describes the mechanisms leading to heterogeneities.

For the estimation of the heat transfer rate to the compartment boundaries ($\dot{Q}_{wall}$), it is necessary to address the heat transfer from the gas phase to the solid. Heat transfer to the compartment elements occurs by convection and radiation. Several experimental studies have measured the different heat transfer components in compartment fires. Most studies use small (order of 1 m) compartments with small openings. A notable example is the experiments by Veloo and Quintiere [64]. Larger compartment fire experiments with larger openings were reported by Lennon and Moore [53] and the heat transfer fields were analysed by Welch et al. [55]. Their results were consistent with those of Veloo and Quintiere [64]. Detailed methodologies to assess both forms of heat transfer have been developed for zone models that include multiple compartments [65] but that remain restricted to small compartments with small openings. The only generalised model that includes all compartment geometries was developed by Jowsey [66] who established the different heat transfer regimes covered through a broad range of velocities and optical thickness. Other simplified methodologies include the adiabatic surface temperature formulation. The adiabatic surface temperature converts radiative and convective heat transfer to a single temperature. This conversion requires a single temperature for the sources of heat along with defined heat transfer coefficients (e.g., convective heat transfer coefficient) [67]. When assuming an optically-thick gas medium during the heating phase, a single gas temperature defines both radiative and convective heat transfer from the compartment gases. Thus, the heat flux to compartment elements in a post-flashover compartment fire is generally associated with the temporal evolution of the compartment gas temperature (T_g).

3.2. Cooling phase

Energy considerations as shown in Equation (2) can also be expressed for the cooling phase, as shown in Fig. 4. The exchange of gases at the compartment opening (i.e., inflow and outflow) plays a key role in the cooling phase, and the difference ($\dot{Q}_{flow,out} - \dot{Q}_{flow,in}$) has to be considered. In addition, the compartment linings gradually cool down and the heat transfer $\dot{Q}_{wall}$ flows from the linings into the compartment gases (i.e., it has a negative value). If the compartment is once again assumed to have a homogeneous temperature, for the cooling phase, Equation (1) can be written as follows:

$$\frac{dQ_{CV}}{dt} = \dot{Q}_{flow,in} - \dot{Q}_{flow,out} + \dot{Q}_{wall} \tag{3}$$

As for the heating phase, the presented differential equation can be solved by adopting different assumptions and simplifications. The compartment gas temperature is primarily governed by advection into and out of the enclosure and the thermo-physical material properties of the compartment linings.

During the heating phase, heat exchange by the flow at the opening is dominated by the static pressure difference between the compartment (hot) and the external environment (cold). In this case, the mass flow rate through a vertical opening (and resulting energy transfer) can be estimated using simple formulas and typical flow velocities are in the order of a few meters per second [59]. During the cooling phase, the temperature difference between the hot compartment linings and the cold air results in natural convection. By considering buoyancy as the dominant force, the velocity of these convective flows can be approximated as $\sqrt{gH}$, taking the compartment height H [m] as characteristic length and g as the gravitational acceleration (9.81 m/s^2). Considering typical compartment heights in the order of a few meters, the characteristic velocity can again be estimated to be of the order of a few meters per second. This corresponds to a characteristic residence time (t_k [s]) in the order of a few seconds [68]. Therefore, the convective cooling of the control volume is typically a very rapid phenomenon.

The compartment elements gradually cool down. The rate of cooling depends on the individual element's physical and thermal properties as well as the convective velocity. A characteristic time for this process can be estimated from the expression of the thermal propagation depth (L_{th} [m]) [69]. Accordingly, the characteristic time (t_k [s]) is proportional to L_{th}^2/α, where α [m^2/s] is the thermal diffusivity of the compartment linings. For typical construction materials, this value can be estimated to be in the order of hours.

This confirms that, after flames quench, the entire cooling process of the compartment elements is much slower than the cooling of the gases in the control volume. After a rapid transition period, the smoke inside the compartment is released and fresh air continuously enters the

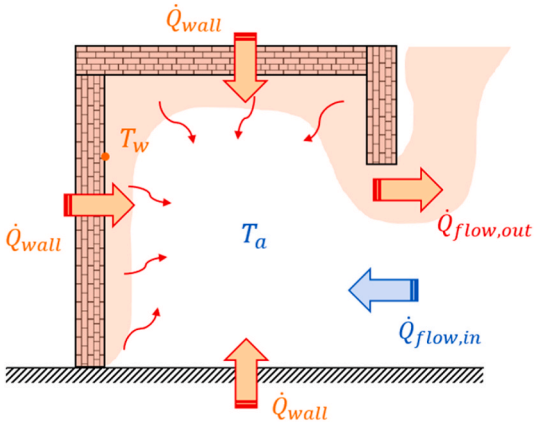

Fig. 4. Side view schematisation of cooling phase.

enclosure through the opening and leaves carrying energy from the compartment elements. The gases inside the compartment quickly become optically thin and radiative exchange between gas and the solids can be considered negligible. A possible simplification, given the short time scales associated with advection, is to assume that the gas temperature is that of ambient ($T_g \approx T_a$). This eliminates the need for Equation (3) and allows simply to estimate $\dot{Q}_{wall}$ using a convective heat transfer coefficient and radiative exchange between the surfaces of the enclosure. This will be explored in Section 5.2.

As in the heating phase, the concept of adiabatic surface temperature [67] can be applied to lump the thermal boundary conditions into a single temperature. However, in the cooling phase, the theoretical adiabatic surface temperature cannot be readily interpreted as corresponding to a physical gas temperature because of the significantly different contributions of convection and radiation.

4. Thermal boundary conditions and compartment fire tests

The literature review highlighted that engineering tools and models for natural fires are generally based on the outcomes of large-scale fire tests. In fire tests, thermocouples of various types and sizes are typically employed with the intention of measuring the evolution of the gas temperature within the compartment during heating and cooling without a clear consideration of the distinction between convective and radiative heat exchanges. However, as described in Section 3.2, during the cooling phase, there is a clear difference between the compartment's gas temperature and the linings' surface temperature. This distinction is not captured by current measurements because the thermocouples are strongly influenced by radiation from the hot compartment linings (see Fig. 5). During cooling the gas phase is optically thin, so to obtain the gas phase temperature, significant corrections for radiation are necessary [55,70,71]. Without a precise correction, thermocouples provide an estimation of the combined effects of the gas phase temperature and the radiative heat being transferred from the surface of the compartment linings. The effect of radiative exchange with the linings increases in importance when thermocouples of larger characteristic dimensions are used, like in the BRE Cardington fire tests [53,55] or in the case of plate thermometers.

Confusion on the definition of the thermal boundary conditions during the cooling phase has nevertheless prevailed. The cooling phase is normally characterised by a parabolic/exponential decreasing branch matched to measured temperatures, see Fig. 1 [39,53,72–75]. Gas temperatures measured using thermocouples have led to various formulations of the cooling phase in engineering models like the Swedish fire curves [39,40]. These temperatures have been interpreted as an opaque gas phase temperature for heat transfer calculations, nevertheless, there is no evidence of appropriate corrections for radiative exchange between the thermocouple and the linings. In contrast, when a radiative correction has been implemented [55], it has been demonstrated that the correction is negligible when the gas phase is optically thick but extremely important when it is optically thin, like in the cooling phase. The lack of comprehensive research studies on this topic has allowed for highly simplified models to prevail despite being frequently criticised [41–43].

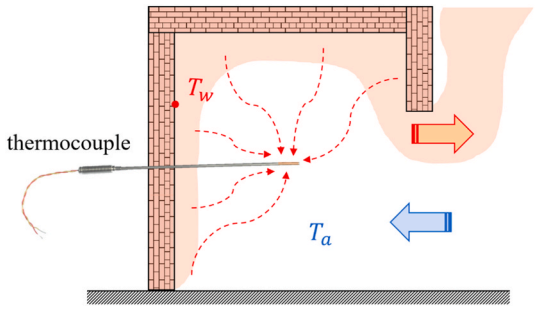

Fig. 5. Schematisation of using a thermocouple to estimate the fire conditions during the cooling phase.

5. Simplified numerical model

Based on the considerations and energy balance equations presented in Section 2 on the heating and cooling phases of natural fires, a simplified numerical model is formulated here. This model aims at estimating the thermal conditions inside a compartment (as any other internal compartment element) during a natural fire, with a special focus on the evolution of the cooling phase. In particular, special attention is paid to the temperature evolution of the inner gases and linings surface within the compartment.

5.1. Heating phase

Within the scope of this research study, the fire heating phase (growth and fully-developed) is estimated according to the Eurocode parametric fire curves, currently the most widely adopted methodology, where the temperature history can be calculated starting from a few input parameters, namely the fuel load density, compartment geometry and characteristics (i.e., ventilation and linings' thermal inertia) [4,5,7,8,10,11,14,21,36,43].

As a result, a temperature-time curve of the compartment gases (T_g) during the heating phase is obtained. In the case of Eurocode parametric fire curves, this temperature can be used as a thermal boundary condition. This is appropriate because for optically thick smoke including the effect of the radiation coming from the heated compartment linings is not necessary, and a single gas temperature controls both convection and radiation heat transfer to the compartment elements [55]. The boundary condition can therefore be defined as:

$$\dot{Q}_{wall} = A_w h_c \left(T_g - T_w\right) + A_w \varepsilon_w \sigma \left(T_g^4 - T_w^4\right) \tag{4}$$

where A_w [m^2] is the compartment linings surface, ε_w [−] is the linings emissivity, and σ is the Stefan–Boltzmann constant (5.67 × 10^{-8} W/m^{2}K^4). Assuming an optically thick smoke, the compartment gases emissivity is not included in the expression, as it is assumed equal to 1. The constant value of 35 W/m^{2}K for natural fire models recommended by Eurocode is used for the convective heat transfer coefficient h_c [36]. This value is an object of intense discussion, underlying the fact that the low velocities assumed in the compartment during the fire fully-developed phase should lead to lower values (values above 25 W/m^{2}K are typically considered to relate to forced convection) [54]. However, given the high temperatures and radiation-dominated heat transfer, the convective heat transfer coefficient has a limited impact during the heating phase.

The end of the fully-developed phase (t_{max} [s]) is a function of the compartment fuel load density (q''_f [MJ/m^2]), opening factor (O [m$^{0.5}$]) and resulting burning rate ($\dot{m}''_f$ [kg/s]). For ventilation-controlled fires, the burning rate can be calculated from the opening factor using Kawagoe's correlation [54]. The opening factor (O [m$^{0.5}$]) is usually expressed as:

$$O = \frac{A_o \sqrt{H_o}}{A_t} \tag{5}$$

where H_o [m] and A_o [m^2] are the compartment opening height and surface area, and A_t [m^2] is the total surface area of the compartment enclosure.

Under the assumption that the total fuel load is consumed during the heating phase (fully-developed fire) and a steady state burning rate, the following expression can be derived to obtain the commonly used expression for the time to burnout:

$$q''_f = \Delta H_c \int_0^{t_{max}} \dot{m}''_f \, \mathrm{d}t \tag{6}$$

$$t_{max} = \frac{q''_f}{\Delta H_c \, \dot{m}''_f} \tag{7}$$

where ΔH_c [MJ/kg] is the fuel effective heat of combustion. In order to consider a consistent heating period, it is important to introduce these equations. However, this part of the solution will not be implemented any further, since similar empirical expressions can be found in various methodologies, like the Eurocode parametric fire curves [36,41].

Using these thermal boundary conditions, the evolution of the surface and in-depth temperatures of the compartment linings can be estimated until the end of the heating phase (here burnout, since all fuel is assumed consumed in the heating phase). The temperatures are calculated using a simplified finite-difference conductive heat transfer model (explicit scheme) [69].

5.2. Cooling phase

Given the description of the cooling phase in Section 3.2, the compartment environment is assumed to be an optically thin, smoke-free, environment and the temperature of the gas phase is assumed to be that of ambient (T_a, i.e. outside). The temperatures of all compartment surfaces evolve due to convective cooling by the gas inside the compartment, as well as by radiation exchange between the various compartment elements. The boundary condition for a specific compartment element (j) of surface temperature $T_{w,j}$ and area $A_{w,j}$ for the cooling phase can thus be written as:

$$\dot{Q}_{wall,j} = A_{w,j} h_{c,j} \left(T_a - T_{w,j}\right) + A_{w,j} \sum_{i=1}^{n} F_{ij} \bar{\varepsilon} \sigma \left(T_{w,i}^4 - T_{w,j}^4\right) \tag{8}$$

where F_{ij} [−] is the view factor between the specific compartment element (j) and another compartment element (i), and $\bar{\varepsilon}$ [−] is the effective emissivity ($\bar{\varepsilon} = 1/[(1-\varepsilon_i)/\varepsilon_i A_i + 1/A_i F_{ij} + (1-\varepsilon_j)/\varepsilon_j A_j]$) [69]. The total value can be estimated by summing the contribution of all the single elements within the compartment. This formulation assumes that the view factor to the outside is small.

With regards to the conduction heat transfer, the same simplified finite-difference conductive heat transfer model can be used as in the heating phase. However, in the case of compartment elements characterised by different thermo-physical properties, the heat transfer $\dot{Q}_{wall,j}$ in the cooling phase needs to be estimated for each element.

Different from the heating phase, the estimation of the convective heat transfer coefficient (h_c) has a key role in the quantification of the thermal boundary conditions during the cooling phase. Convective heat transfer has a primary importance because it controls the cooling of the compartment linings, and therefore the heat fluxes within the compartment. Typical values for free convection are in the range of 5–25 W/m^{2}K [54]. Considering the compartment walls as vertical hot flat surfaces subjected to natural free convection, empirical correlations based on the Nusselt number can be used to obtain a first approximation of the convective heat transfer coefficient [69,76]. It is certain that more refined approaches can be followed, nevertheless, the precision by which the heat transfer coefficient is estimated is not the subject of this study. Further refinements could follow but will require a more detailed characterisation of the regimes being explored as has been done by multiple authors for several specific regimes [55,63,64,66]. Assuming a characteristic length of 1–4 m (assumed as compartment height) and surface temperatures of 200–1200 °C, Fig. 6 shows that the convective heat transfer coefficient has limited variability for these conditions (6.4–7.6 W/m^{2}K). Due to recirculation flows, higher velocities and convective heat transfer coefficients could be expected in the enclosure. However, for simplicity, the convective heat transfer coefficient for the cooling phase is set equal to 7 W/m^{2}K [77].

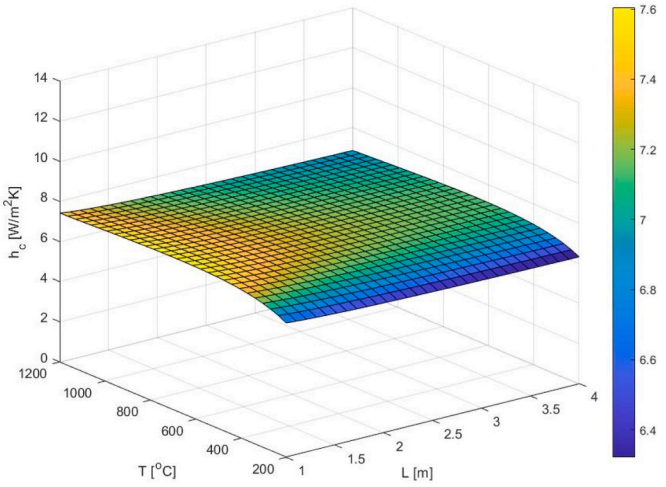

Fig. 6. Convective heat transfer coefficient h_c as a function of characteristic length and surface temperature.

With regards to the radiative heat transfer, the simplified model assumes that rapid cooling of the compartment gases at fuel burnout leads to a transparent (optically thin) environment inside the enclosure. Thus, the surfaces are free to exchange heat. Compartment surfaces can have different linings with different thermal properties. This can result in different surfaces temperatures and thus radiative heat exchange within surfaces. Any precise calculation of the temperature histories within structural elements will require the inclusion of these property differences. This study does not aim to deliver such level of precision, but rather an illustration of the impact of convective cooling. Therefore, as a simplification, all the compartment linings will be assumed to be made of the same material and, given the assumed uniform gas temperature and convection coefficient, therefore will follow identical temperature evolutions. Accordingly, the second term in the right-hand side of Equation (8) can be completely eliminated. However, if the analysis focuses on the thermal evolution of a compartment element that is highly sensitive to the temperature of the surrounding surfaces, the radiation exchange must be included into the calculation. This aspect is discussed in detail in Section 7.2.

6. Modelling results

6.1. Case study

The presented numerical model is analysed to estimate the thermal conditions from a natural fire, with a specific focus on the cooling phase. A case study is defined: a square compartment of 7.5 × 7.5 m^2 in plan, 3 m in height, with an opening factor of 0.04 m$^{0.5}$, a fuel load density per unit floor area of 720 MJ/m^2 and compartment linings with a thermal inertia of 1160 J/m^{2}s$^{0.5}$K (typical value for lightweight concrete), surface emissivity of 0.8, and thickness of 0.20 m. All compartment linings are the same, so heating and cooling rates are the same as well, considering uniform convection coefficients and 1D heat transfer. This case is chosen to provide a heating phase of 1 h similar to the standard fire curve according to the Eurocode parametric fire curves methodology (scaling factor Γ equal to 1) [36]. To solve the simplified numerical model, the spatial discretisation finite-difference conductive heat transfer model inside the linings is set equal to 1 mm and the time step as 0.01 s. It has been confirmed that these settings result in numerical stability. The ambient temperature is specified as 20 °C. With the described assumptions and input parameters, the numerical model enables the evaluation of the temperature-time histories of the compartment gases and linings. These outcomes are shown in Fig. 7, which also

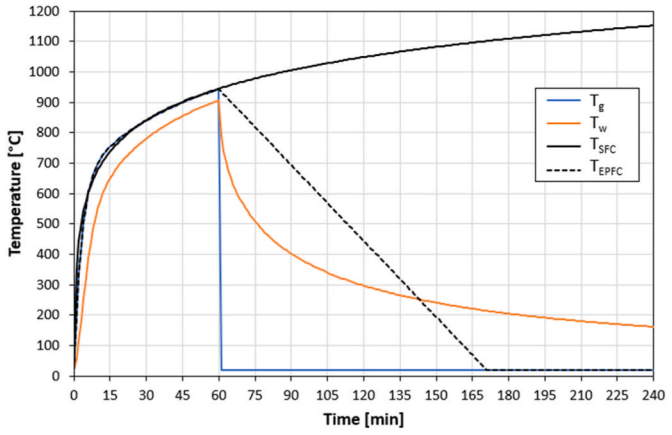

Fig. 7. Evolution of the compartment gases (T_g) and linings surface temperatures (T_w) obtained from the simplified model, compared to the standard fire curve (T_{SFC}) and the corresponding Eurocode parametric fire curve (T_{EPFC}).

reports the ISO 834 standard fire curve and the corresponding Eurocode parametric fire curve. In addition, Fig. 8 reports the calculated heat fluxes of various natures between the compartment gases and linings, and Fig. 9 shows the in-depth temperature profiles within the compartment linings during heating and cooling.

With regards to the heating phase, the gas and linings surface temperatures rapidly increase until they reach a maximum value, achieved at fuel burnout. The gas temperature is higher than the surface temperature, but they follow a very similar trend, defined by the thermo-physical properties of the linings material (i.e., its thermal inertia). In this phase, there is a significant net heat flux entering the compartment linings from the hot gases ($\dot{q}_{net}''$), where the radiative component ($\dot{q}_{rad}''$) dominates the heat transfer compared to the convective ($\dot{q}_{conv}''$) component. The net heat flux absorbed at the linings surface ($\dot{q}_{net}''$) is conducted in-depth into the material ($\dot{q}_{cond}''$), so these fluxes are equal (with opposite sign) at all times.

At fuel burnout, the gas temperature is set to ambient conditions, while the linings surface temperature gradually decreases. This temperature-time curve is characterised by decreasing cooling rates (high for elevated temperatures and low for lower temperatures, see Fig. 7 after 60 min), and it is determined by the convective cooling of the compartment linings surface temperature and their thermo-physical properties. For this example, and given that all the linings are the

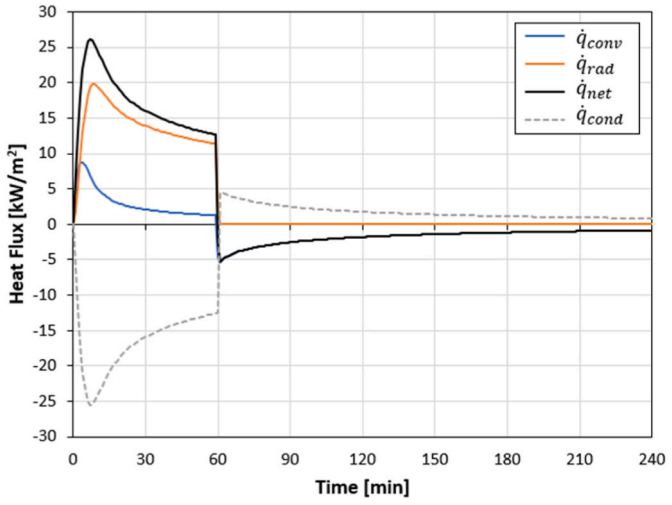

Fig. 8. Evolution of the convective ($\dot{q}_{conv}''$), radiative ($\dot{q}_{rad}''$), net ($\dot{q}_{net}''$), and conductive heat fluxes ($\dot{q}_{cond}''$) between the compartment gases and linings.

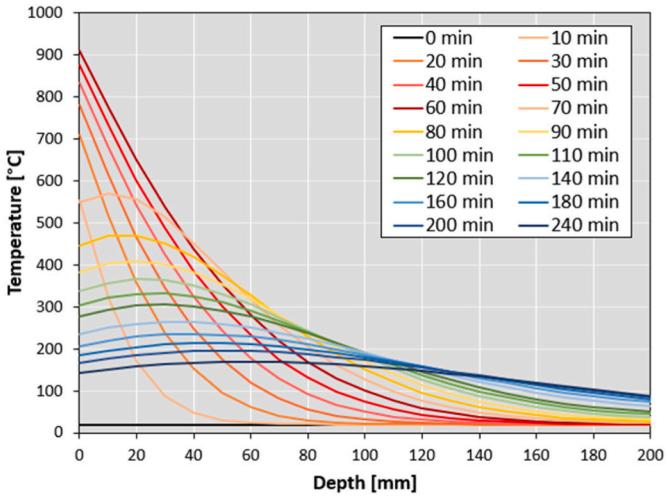

Fig. 9. In-depth temperature profiles within the compartment linings at different instants.

same, the net radiative exchange between them is zero. The radiative heat flux between the gases and linings ($\dot{q}_{rad}''$) also decreases to zero, while all the heat conducted through the linings surface ($\dot{q}_{cond}''$) is transferred to the compartment gases due to surface convective cooling. Fig. 8 highlights how, in the heating and cooling phase, the direction of heat transfer (i.e., signs positive/negative) is opposite. Due to the strong assumption of full fuel consumption in the heating phase (no gradual fire decay phase) and consequent simplification of compartment gases at ambient temperature during the cooling phase, there is a significant discontinuity between the two phases, but the simplified numerical model provides a correct phenomenological description of the compartment conditions during cooling. The results could certainly be improved by including a transient phase that considers the gradual decrease of the fire heat release rate, as well as the gradual cooling of the compartment gases.

6.2. Parametric study

To investigate the influence of various assumptions and input parameters on the numerical model, a parametric study is carried out focusing on the cooling phase. Fig. 10 presents the results obtained from the parametric study on the evolution of the compartment gases and linings surface temperatures with varying convective (cooling) heat transfer coefficient (h_c), opening factor (O), linings' thermal inertia (b), and fuel load density (q_f'').

Fig. 10 highlights how a higher convective (cooling) heat transfer coefficient produces a faster surface cooling. However, the difference between 5 and 10 W/m^{2}K is quite limited. On the other hand, Fig. 10 underlines that the other variables affect the cooling phase in a more significant manner, particularly because they have an important impact on the heating phase. This emphasises how there is a strong relationship between the heating and the cooling phase, and the two phases cannot be fully decoupled. For instance, a higher compartment opening factor generally creates a higher maximum gas temperature at fuel burnout, but a shorter fully-developed fire with a higher heating rate: this leads to a higher compartment linings temperature at the end of the heating phase, reduced thermal penetration depth and faster cooling. As regards the compartment linings material, higher thermal inertia does not affect the fully-developed fire duration, but it results in lower maximum gas temperature (higher convection losses at boundaries), a lower heating rate, and lower compartment linings temperature at burnout. However, in all cases, the surface temperature follows temperature trends similar to each other, even if they start cooling at significantly different

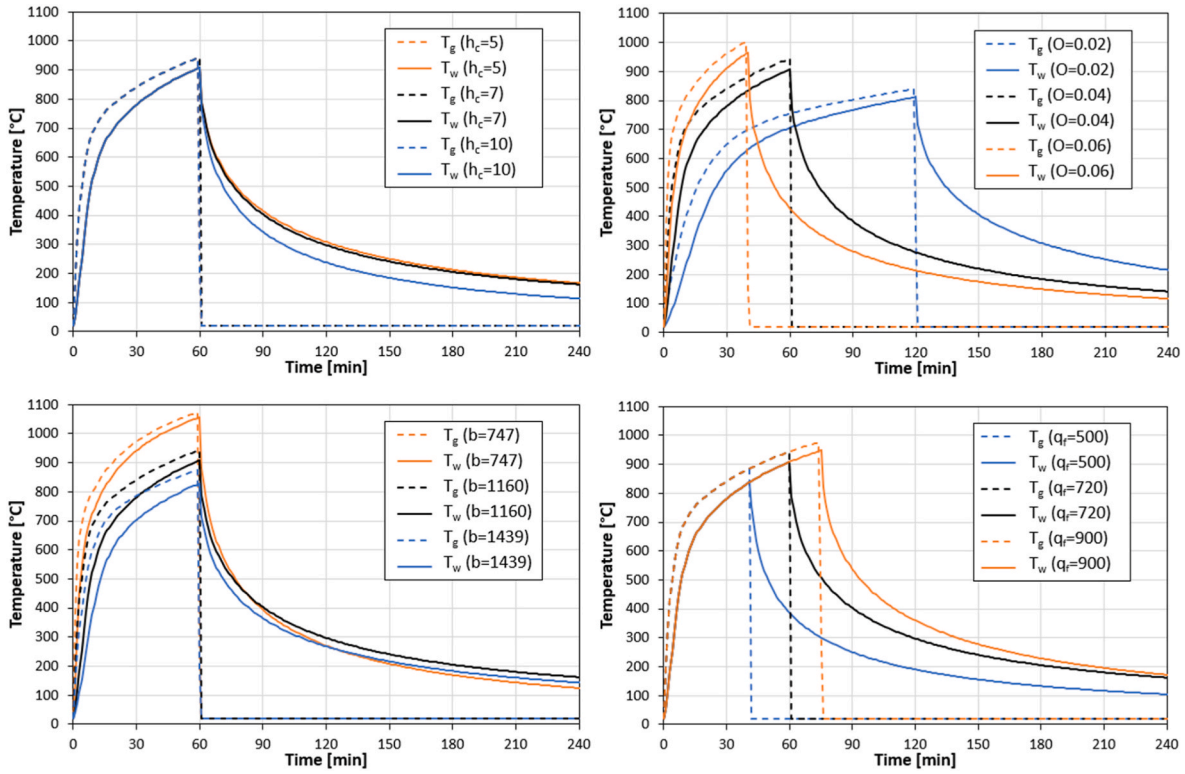

Fig. 10. Parametric study on the evolution of the compartment gases (T_g) and linings surface temperatures (T_W) with varying convective heat transfer coefficient (h_c [W/m^{2}K]), opening factor (O [m$^{0.5}$]), linings' thermal inertia (b [J/m^{2}s$^{0.5}$K]), and fuel load density ($q_f^{'}$ [MJ/m^2]).

temperatures. This is related to the thermal inertia because, similarly to the heating phase, the linings material responds to surface thermal conditions changes according to its thermal inertia: the lower the thermal inertia, the faster the surface responds to a gas temperature change. Finally, a higher compartment fuel load density prolongs the heating phase with the same heating rate, and it leads to a higher maximum gas temperature and compartment linings temperature at burnout. Accordingly, the surface cooling is slower due to the deeper heat penetration. A similar effect can be also created by a larger compartment size, if the compartment opening factor is fixed.

7. Discussion

7.1. Comparison with the eurocode parametric fire curve methodology

The majority of research studies available in the literature that focus on the decay phase and cooling phase effects of the post-flashover compartment fires on structural elements typically define the thermal boundary conditions by the Eurocode parametric fire curves [4,5,7,8,10,11,14,21,43]. The effect of imposing different boundary conditions in the cooling phase becomes evident if the simplified numerical model is compared to the Eurocode parametric fire curves methodology [36].

It is important to highlight that, despite a different common belief, the Eurocode parametric fire curves methodology assumes that the total fire heat is released during the fully-developed phase, therefore the end of this phase corresponds to the beginning of the cooling phase, without any decay phase [56]. Indeed, the duration of the fire fully-developed phase is calculated considering the total fuel load, in analogy with Kawagoe's theory [54]. Accordingly, the temporal evolution of the fire heat release rate underlying the presented simplified model and the Eurocode parametric fire curves is the same.

This section provides a comparison between the model and the Eurocode approach to illustrate any potential differences: the case study discussed in Section 6.1 is solved according to the two methodologies, given identical heating phases.

Fig. 11 first evidences the considerable difference between the evolution of the compartment gases (T_g) and linings surface temperatures (T_w) during the cooling phase following the two methodologies. The linings surface temperature for the simplified model reproduces a classical non-linear cooling down evolution, while the parametric curve shows that linings and gas phase temperature do not differ much. Indeed, the evolution of the linings surface temperature (T_w) according to the Eurocode parametric fire curves methodology was calculated using the prescribed Eurocode thermal boundary conditions starting from the evolution of the compartment gases (T_g) [36].

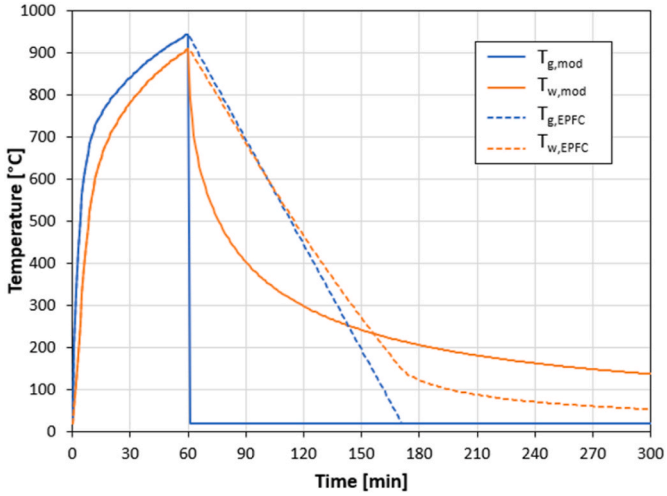

Fig. 11. Compartment gases (T_g) and linings surface temperatures (T_w) according to the simplified model and the Eurocode parametric fire curve methodology.

Similarly, the in-depth temperature profiles within the compartment linings (Fig. 12) and the conductive heat fluxes at the linings surface (Fig. 13) differ significantly. Based on the defined conditions for the cooling phase in the simplified numerical model, the fuel burnout (60 min) corresponds to the beginning of the compartment gases and linings cooling. This can also be confirmed by the positive conductive heat fluxes at the compartment linings surface (heat transfer from solid into gases). In contrast, the Eurocode parametric fire curves methodology imposes thermal boundary conditions that lead to negative heat fluxes for an additional 40 min (until about 100 min). Indeed, for this period following the end of the heating phase, the compartment gas temperature is still higher than the linings surface temperature, causing a net heat flux into the solid. Only when $T_g < T_w$, the compartment linings commence the cooling process with the surrounding environment, yielding positive conductive heat fluxes (refer to Fig. 13). Consequently, the two different thermal boundary conditions lead to an important difference in the in-depth temperature distributions.

To investigate the effects of the thermal boundary conditions defined according to the two methodologies on the thermal energy of the compartment elements, the evolution of the total in-depth thermal energy (per unit area) accumulated within the compartment linings was calculated as:

$$E''_{th}(t) = \int_0^d \rho c_p \Delta T(x,t)\, \mathrm{dx} \tag{9}$$

where ρ is the mass density [kg/m^3], c_p is the specific heat capacity [J/kgK], and $\Delta T(x,t)$ [K] is the time-varying in-depth temperature rise within the thickness of the solid (d [m]). For simplicity and in analogy with the case study described in Section 6.1, the material properties are kept constant.

Fig. 14 underlines how, during the cooling phase, the total thermal energy differs significantly between the two methodologies. With regards to the simplified model, the end of the heating phase corresponds to the beginning of thermal energy decrease, as the model assumes fuel burnout and convective cooling after this point. On the contrary, in the case of the Eurocode parametric fire curves, the end of the heating phase does not constitute the end of thermal gain for the solid. For these specific conditions, there is an additional thermal gain in the system during the cooling phase, until when the conductive heat flux at the compartment linings surface is positive, hence only when $T_g < T_w$. Given that the fire has burnt out, this is physically incorrect and represents an unnecessary over-dimensioning of the thermal load. In the Eurocode case, the thermal state (i.e. total in-depth thermal energy) at

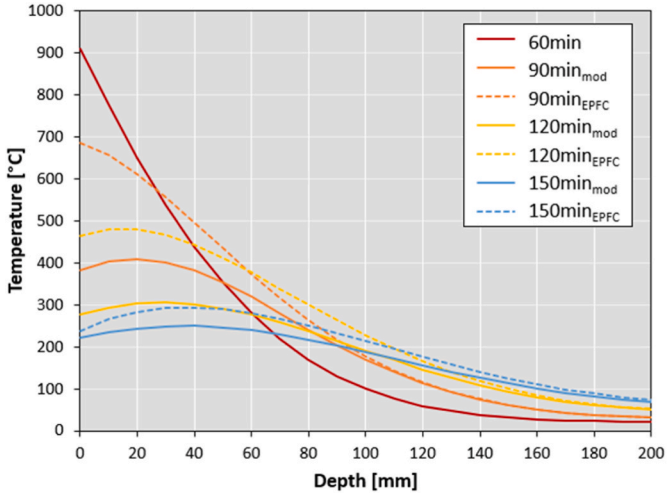

Fig. 12. In-depth temperature profiles within the compartment linings at different instants according to the simplified model and the Eurocode parametric fire curve methodology.

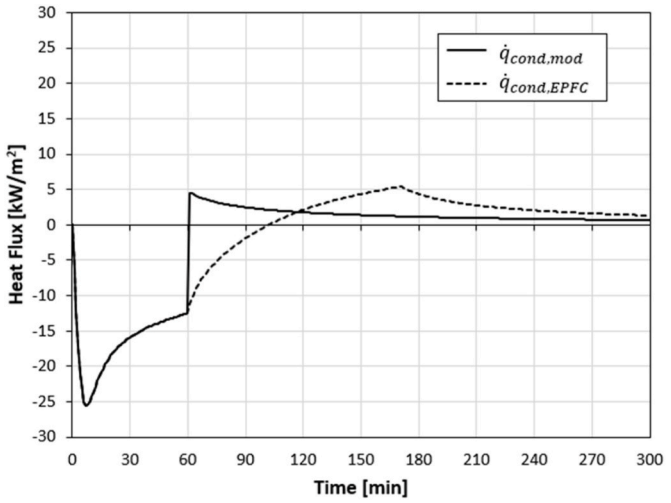

Fig. 13. Conductive heat fluxes ($\dot{q}''_{cond}$) at the compartment linings surface according to the simplified model and the Eurocode parametric fire curve methodology.

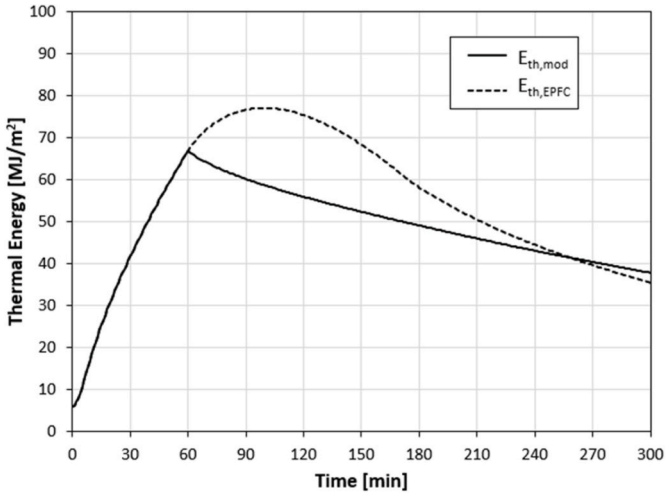

Fig. 14. Total in-depth thermal energy within the compartment linings according to the simplified model and the Eurocode parametric fire curve methodology.

the end of the heating phase is reached again at about 150 min, creating a "cooling delay" of about 1.5 h compared to the simulation results from the simplified model. After this point, the cooling is faster than the simplified model, due to the contribution of the imposed radiation losses and larger convective (cooling) heat transfer coefficient (35 W/m^{2}K vs. 7 W/m^{2}K).

This analysis highlighted the impact of the definition of the thermal boundary conditions and the significant differences between the two approaches. It has been shown how, according to the Eurocode parametric fire curves methodology, which does consider fuel burnout at the end of the heating phase, the end of the heating phase does not correspond to the end of thermal gain within the solid. By defining these thermal boundary conditions, the thermal energy in the solid continues to grow for a significant amount of time. This leads to a delay in the onset of cooling of the compartment elements and, possibly, an overestimation of the impact of post-flashover fires. Indeed, if the duration of the heating phase is estimated assuming that all the fuel within the compartment is consumed at the end of the heating phase (i.e., burnout), it is incorrect to consider an additional thermal gain during the cooling phase.

It is recalled that the present model: (i) does not consider a decay phase, thus releases all energy as contained in the combustible materials during the heating period, (ii) assumes the absorptivity of the gas to be zero and its temperature to be equal to ambient during the cooling phase, and (iii) fully captures the radiative heat exchange between surfaces, assuming a uniform temperature for each surface. Because of these simplifications, the temperature evolution of the structural elements will introduce errors, but there is no heat added into the compartment after completion of fuel burnout, thus avoiding a non-physical heat flux into the structure.

7.2. Including the radiative heat exchange

In the presented simplified model, no radiative heat exchange has been estimated between the compartment elements during the cooling phase because, for simplicity, equal surface temperatures were assumed for all compartment surfaces. To obtain a more realistic result, the radiation feedback and heat transfer during the cooling phase should be included, particularly considering how various compartment elements (and surfaces) would cool down and exchange heat through radiation within the enclosure. To do so, the thermal boundary conditions described in Equation (8) (final term) must be solved considering the view factor, temperature and area of each single element within the compartment. Thus, gas phase and radiative heat transfer between the various compartment surfaces (e.g., structural elements and linings) need to be determined in a coupled manner. This process might be computationally intensive as it requires solving the entire coupled heat transfer problem at each instant in time (i.e., surface and in-depth temperatures, as well as thermal boundary conditions, for each element within the compartment). This approach might prove impractical for complex building geometries and compartments composed of multiple linings materials. It is therefore useful to explore a simplified approximation for the evolution of cooling compartment surfaces in order to estimate and incorporate the radiative heat exchange.

Given that convective and radiative heat transfer are much faster than conductive cooling of the solid, convection and radiation can be treated as steady processes, while conductive cooling of the solid remains the only transient process. Convection has already been decoupled by assuming a constant convective heat transfer coefficient, while quasi-steady radiative heat exchange can be estimated from a representative temperature evolution of the compartment linings surface.

An analytical expression of the cooling branch can be obtained by adjusting the well-known analytical solution for transient conduction in a semi-infinite solid with convective thermal boundary conditions through a variable transformation [69]. The analytical solution is typically used for heating or cooling of semi-infinite solids, given a convective heat transfer coefficient, ambient temperature, and initial temperature. In this case, the solution is altered to estimate the surface cooling of the compartment linings, starting from a given convective heat transfer coefficient and in-depth temperature profile (i.e., achieved at the end of the heating phase). As in the numerical model, the convective (cooling) heat transfer coefficient can be set equal to 7 W/m^{2}K. On the other hand, the thermal gradient within the compartment linings at the end of the heating phase is defined as a function of the thermal penetration depth (L_{th} [m]):

$$L_{th} = n\sqrt{\alpha t_k} \tag{10}$$

where n [−] is a multiplication factor for the estimation of the thermal penetration depth (typically 4 for most applications [69]), α [m^2/s] is the thermal diffusivity of the compartment linings, and t_k [s] is the characteristic time, assumed equal to the duration of the heating phase [69]. The extremes of the thermal gradient are defined by the compartment linings surface temperature at the end of the heating phase (maximum temperature) and ambient temperature (see Fig. 15). To obtain a simple analytical solution, the thermal gradient is assumed to be linear to avoid a second-order derivation of the transformation equation different from zero. The transformed solution is obtained by removing the convective cooling contribution from the initial thermal gradient estimated at the end of the heating phase. The derivation of the analytical solution and the variable transformation are explained in detail in Appendix A.

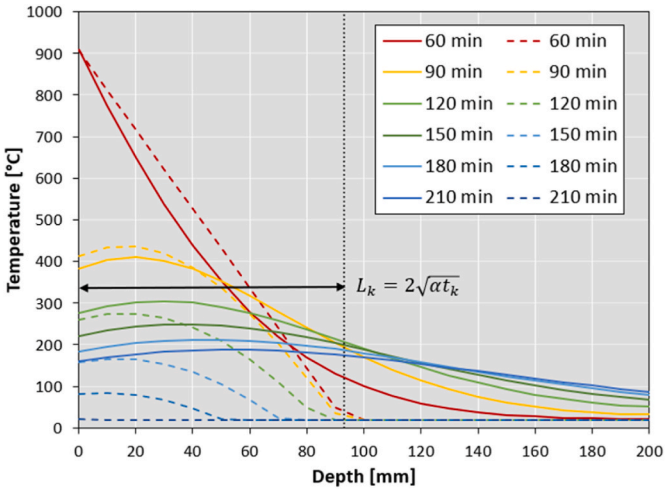

Fig. 15. Comparison between the in-depth temperature profiles within the compartment linings during cooling obtained using the numerical model (continuous lines) and the analytical approximation (n = 2, dashed lines).

Accordingly, starting from the compartment linings surface temperature at the end of the heating phase and knowing the thermophysical properties of the compartment linings, the thermal gradient at the end of the heating phase can be estimated according to the thermal penetration depth L_{th} (Equation (10)). Starting from this gradient, the thermal gradient within the compartment linings is decreased by adding the convective cooling contribution estimated according to the analytical solution with variable transformation (refer to Appendix A). This methodology produces an approximation of the surface cooling of the compartment linings, as shown in Fig. 16. Different values of n produce various levels of accuracy compared to the temperature curve obtained from the numerical model. This aspect is closely related to the approximation of the thermal gradient within the compartment linings at the end of the heating phase. As highlighted in Fig. 15, this thermal gradient acts as a starting point for the approximation of the in-depth temperatures during cooling, and it directly depends on n because it

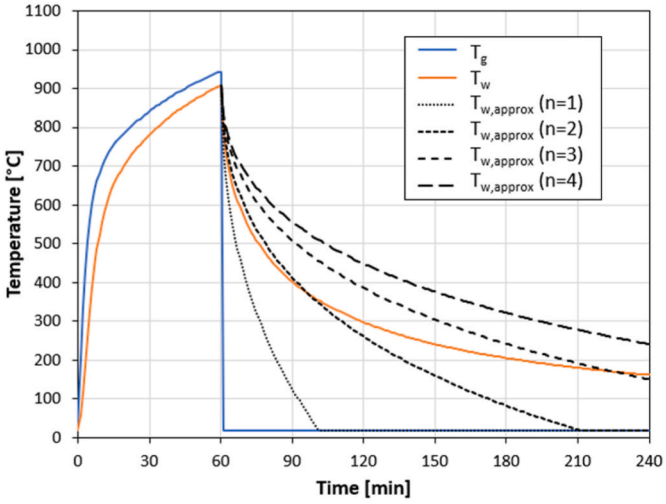

Fig. 16. Surface cooling of compartment linings for different n obtained using the analytical approximation (dashed lines).

defines the thermal penetration depth, hence its slope. Fig. 16 evidences how higher values of n produce slower cooling due to the deeper thermal penetration depth and a less steep thermal gradient within the solid. The choice of the value n is key because it generates an over- or under-estimation of the temperature evolution of the compartment linings surface and this choice strongly depends on the application of the presented methodology. For structural fire engineering problems, the over-estimation of the thermal exposure generally produces a conservative solution. However, it is also important to estimate realistic thermal conditions and to consider which temperature ranges are relevant for the construction material and structural system under analysis. For instance, the case study presented in Fig. 16 ($n = 2$) offers a good approximation of the cooling branch for temperatures above 350 °C.

In general, this methodology offers an analytical approximation for the surface cooling of the compartment linings, which can be used to estimate the radiative heat exchange to an element inside the compartment (Equation (8)) during the cooling phase of a post-flashover compartment fire.

8. Conclusions

The current study focused on describing the main characteristics of the cooling phase of post-flashover compartment fires, evidencing the differences in the manner the thermal boundary conditions are expressed when contrasted with the heating phase. The heating phase is typically characterised by optically thick smoke with high temperatures and the thermal boundary conditions can be correctly approximated by a single (gas) temperature. After fuel burnout, the compartment gases quickly become optically thin and tend to ambient temperature, while the compartment linings gradually cool down. The different characteristic time scales of convective cooling of the compartment, convective cooling of the solid, radiative heat exchange between solid surfaces and conductive heat transfer within the compartment require a more detailed mathematical representation of the thermal boundary conditions.

Accordingly, a simplified numerical model was formulated to estimate the thermal conditions during the cooling phase. The heating phase is defined according to the Eurocode parametric fire curves methodology, while the thermal boundary conditions during the cooling phase are defined by a detailed analysis of all heat transfer modes and simplifications consistent with the different time scales. A constant convective (cooling) heat transfer coefficient can be defined to characterise natural convective cooling of the compartment linings, while the evolution of the linings surface temperature characterises radiative heat exchange between the compartment linings and the construction element under analysis. The time-history of the linings surface temperature can be also approximated transforming the well-known analytical solution for transient conduction in a semi-infinite solid.

The application of the numerical model evidenced the importance of defining the thermal boundary conditions of the compartment structure during the cooling phase. Moreover, a parametric study underlined how the heating and the cooling phases are closely related and cannot be fully decoupled. Indeed, key parameters (convective heat transfer coefficient, opening factor, linings material and fuel load density) that have an important impact on the heating phase also affect the cooling phase in a significant manner.

The simplified model suggests various simplifications to estimate the convective and radiative heat transfer during the cooling phase of post-flashover compartment fires. In particular, it shows how the system starts cooling immediately after burnout. In contrast, the thermal boundary conditions (based on a single temperature) recommended by the Eurocode parametric fire curves methodology lead to energy and temperature increase in the solid beyond fuel burnout and therefore an unphysical delay in the onset of cooling of the compartment elements. This can possibly cause an over-estimation of the impact of post-flashover fires on load-bearing elements.

The presented simplified approach was proposed to provide a first example of how the cooling phase of post-flashover compartment fires can be thermally characterised. Indeed, the present study does not provide a distinction between the decay phase and the cooling phase of post-flashover compartment fires, and it actually delivers an averaged representation of the different surface temperatures of a compartment at the limit where all combustible materials are consumed during the heating phase. This is the case because it relies on two important simplifications: the end of the fully-developed phase is assumed as fuel burnout and therefore the beginning of the cooling phase, and during the cooling phase the compartment gases are assumed to have an absorptivity of zero and to remain at ambient temperature. This is the reason for the evident discontinuity in the compartment gas temperature evolution at the (sudden) transition between the heating and cooling phase. Increasing the complexity and challenging the model assumptions (e.g. introducing a decay phase for the fire heat release rate) will be addressed in future work, also investigating existing experimental data from large-scale compartment fire tests.

CRediT authorship contribution statement

Andrea Lucherini: Writing – original draft, Visualization, Project administration, Methodology, Investigation, Funding acquisition, Formal analysis, Data curation, Conceptualization. **Balša Jovanović:** Writing – review & editing, Methodology, Investigation, Formal analysis, Data curation, Conceptualization. **Jose L. Torero:** Writing – review & editing, Supervision, Methodology, Conceptualization. **Ruben Van Coile:** Writing – review & editing, Supervision, Methodology, Funding acquisition, Conceptualization. **Bart Merci:** Writing – review & editing, Supervision, Methodology, Funding acquisition, Conceptualization.

Declaration of competing interest

The authors declare that they have no known competing financial interests or personal relationships that could have appeared to influence the work reported in this paper.

Data availability

Data will be made available on request.

Acknowledgements

The authors would like to thank the scientific support kindly offered by the Structural Fire Engineering (SFE) and the Fire Safety Science and Engineering (FSSE) research teams at Ghent University. Dr Lucherini would also like to gratefully acknowledge the financial support for the FRISSBE project within the European Union's Horizon 2020 research and innovation programme (GA 952395) and for the FIReSafeTimber project within the European Union's Horizon Europe Marie Skłodowska-Curie Postdoctoral Fellowship (GA 101064840).

APPENDIX A

Analytical solution [69]

General transient conduction problem

$$\frac{\partial T}{\partial t} = \alpha \frac{\partial^2 T}{\partial x^2}$$

Boundary conditions for semi-infinite solid with surface convection (convective heat transfer coefficient h_c and ambient temperature T_a) and initial temperature T_i.

$$\begin{cases} \text{for } t = 0, T = T_i \\ \text{for } t > 0 \text{ and } x = 0, -k\dfrac{\partial T}{\partial x} = h_c[T_a - T(0,t)] \\ \text{for } t > 0 \text{ and } x \to \infty, T = T_i \end{cases}$$

Analytical solution for in-depth temperature evolution $T(x,t)$ at time t and depth x.

$$\frac{T(x,t) - T_i}{T_a - T_i} = \operatorname{erfc}\left(\frac{x}{2\sqrt{\alpha t}}\right) - \left[\exp\left(\frac{h_c x}{\lambda} + \frac{h_c^2 \alpha t}{\lambda^2}\right)\right]\left[\operatorname{erfc}\left(\frac{x}{2\sqrt{\alpha t}} + \frac{h_c\sqrt{\alpha t}}{\lambda}\right)\right]$$

Analytical solution for surface temperature evolution $T(0,t)$ at time t.

$$T(0,t) = T_i + (T_a - T_i)\left[1 - \exp\left(\frac{h_c^2 \alpha t}{\lambda^2}\right)\operatorname{erfc}\left(\frac{h_c\sqrt{\alpha t}}{\lambda}\right)\right]$$

Variable transformation

Variable transformation: analytical solution $T(x,t)$ for semi-infinite solid with surface convection and initial temperature subtracted by a known function $f(x)$, which represents the initial thermal condition (i.e., in-depth thermal gradient achieved at the end of the heating phase)

$$\overline{T}(x,t) = T(x,t) - f(x)$$

Boundary conditions of the function $f(x)$.

$$f(x) = \begin{cases} x = 0, 0 \\ x \to \infty, -T_{s,max} + T_a \end{cases}$$

Function $f(x)$, with first and second derivative, defined based on the ambient temperature T_a, the maximum surface temperature $T_{s,max}$ (achieved at the end of heating phase) and characteristic thermal penetration depth L_{th} (i.e., define the in-depth thermal gradient achieved at the end of the heating phase)

$$f(x) = \frac{T_a - T_{s,max}}{L_{th}} x$$

$$\frac{\partial f(x)}{\partial x} = \frac{T_a - T_{s,max}}{L_{th}}$$

$$\frac{\partial^2 f(x)}{\partial x^2} = 0$$

Characteristic thermal penetration depth L_{th} defined based on the material thermal diffusivity α, a characteristic time t_k (heating time), and a multiplication factor n (discussed in Section 7.2):

$$L_{th} = n\sqrt{\alpha t_k}$$

Derivation of transformed variable

$$\frac{\partial T}{\partial t} = \frac{\partial \overline{T}}{\partial t}$$

$$\frac{\partial T}{\partial x} = \frac{\partial \overline{T}}{\partial t} + \frac{\partial f(x)}{\partial x} = \frac{\partial \overline{T}}{\partial t} + \frac{T_a - T_{s,max}}{L_{th}}$$

$$\frac{\partial^2 T}{\partial x^2} = \frac{\partial}{\partial x}\left(\frac{\partial \overline{T}}{\partial x} + \frac{\partial f(x)}{\partial x}\right) = \frac{\partial^2 \overline{T}}{\partial x^2} + \frac{\partial^2 f(x)}{\partial x^2} = \frac{\partial^2 \overline{T}}{\partial x^2}$$

Derivation of boundary conditions for $t > 0$ and $x = 0$.

$$-\lambda\frac{\partial \overline{T}}{\partial x} = h_c[\overline{T}(0) + f(0) - T_a] + \frac{\partial f(x)}{\partial x}$$

$$-k\frac{\partial \overline{T}}{\partial x} = h_c\left\{\overline{T}(0) - \left[T_a - \frac{\lambda}{h_c}\frac{\partial f(x)}{\partial x}\right]\right\} = h_c\left\{\overline{T}(0) - \left[T_a - \frac{\lambda}{h_c}\frac{T_a - T_{s,max}}{n\sqrt{\alpha t_k}}\right]\right\}$$

Analytical solution with variable transformation

Transient conduction problem with transformed variable

$$\frac{\partial \overline{T}}{\partial t} = \alpha \frac{\partial^2 \overline{T}}{\partial x^2}$$

Boundary conditions of transient conduction problem with transformed variable

$$\begin{cases} \text{for } t = 0, \overline{T} = T_{s,max} \\ \text{for } t > 0 \text{ and } x = 0, -k\dfrac{\partial \overline{T}}{\partial x} = h_c(\overline{T} - T^*) \text{ with } T^* = T_a - \dfrac{k}{h_c}\dfrac{T_a - T_{s,max}}{n\sqrt{\alpha t_k}} \\ \text{for } t > 0 \text{ and } x \to \infty, \overline{T} = T_{s,max} \end{cases}$$

Analytical solution for in-depth temperature evolution T(x,t) at time t and depth x

$$\frac{\overline{T}(x,t) - \overline{T}_i}{\overline{T}_a - \overline{T}_i} = \operatorname{erfc}\left(\frac{x}{2\sqrt{\alpha t}}\right) - \left[\exp\left(\frac{h_c x}{\lambda} + \frac{h_c^2 \alpha t}{\lambda^2}\right)\right]\left[\operatorname{erfc}\left(\frac{x}{2\sqrt{\alpha t}} + \frac{h_c\sqrt{\alpha t}}{\lambda}\right)\right]$$

$$\begin{cases} \overline{T}_i = T_{s,max} \\ \overline{T}_a = T_a - \dfrac{k}{h_c}\dfrac{T_a - T_{s,max}}{n\sqrt{\alpha t_k}} \end{cases}$$

$$T(x,t) = \overline{T}(x,t) + f(x)$$

Analytical solution for surface temperature evolution T(0,t) at time t

$$\overline{T}(0,t) = \overline{T}_i + (\overline{T}_a - \overline{T}_i)\left[1 - \exp\left(\frac{h_c^2 \alpha t}{\lambda^2}\right)\operatorname{erfc}\left(\frac{h_c\sqrt{\alpha t}}{\lambda}\right)\right]$$

$$\begin{cases} \overline{T}_i = T_{s,max} \\ \overline{T}_a = T_a - \dfrac{\lambda}{h_c}\dfrac{T_a - T_{s,max}}{n\sqrt{\alpha t_k}} \end{cases}$$

$$T(0,t) = \overline{T}(0,t)$$

References

[1] A.H. Buchanan, A.K. Abu, Structural Design for Fire Safety, second ed., John Wiley & Sons, 2017 https://doi.org/10.1002/9781118700402.

[2] A. Law, L.A. Bisby, The rise and rise of fire resistance, Fire Saf. J. 116 (2020) 103188, https://doi.org/10.1016/j.firesaf.2020.103188.

[3] J. Gales, B. Chorlton, C. Jeanneret, The historical Narrative of the standard temperature–time heating Curve for structures, Fire Technol. 57 (2021) 529–558, https://doi.org/10.1007/s10694-020-01040-7.

[4] T. Gernay, J.M. Franssen, A performance indicator for structures under natural fire, Eng. Struct. 100 (2015) 94–103, https://doi.org/10.1016/j.engstruct.2015.06.005.

[5] T. Thienpont, R. Van Coile, R. Caspeele, W. De Corte, Burnout resistance of concrete slabs: probabilistic assessment and global resistance factor calibration, Fire Saf. J. 119 (2021) 103242, https://doi.org/10.1016/j.firesaf.2020.103242.

[6] T. Gernay, V. Kodur, M.Z. Naser, R. Imani, L. Bisby, Concrete structures, in: International Handbook of Structural Fire Engineering, The Society of Fire Protection Engineers Series, LaMalva K., Hopkin D, 2022, https://doi.org/10.1007/978-3-030-77123-2.

[7] T. Gernay, J.-M. Franssen, F. Robert, R. McNamee, R. Felicetti, P. Bamonte, S. Brunkhorst, S. Mohaine, J. Zehfuß, Experimental investigation of structural failure during the cooling phase of a fire: Concrete columns, Fire Saf. J. 134 (2022) 103691, https://doi.org/10.1016/j.firesaf.2022.103691.

[8] B. Jovanović, A. Lucherini, R. Van Coile, B. Merci, R. Caspeele, E. Reynders, G. Lombaert, Effects of the fire decay phase on the bending capacity of a fire-exposed reinforced-concrete slab, in: Proceedings of the 7th International Conference on Applications of Structural Fire Engineering, ASFE'21), Ljubljana, Slovenia, 2021.

[9] M.S. Dimia, M. Guenfoud, T. Gernay, J.M. Franssen, Collapse of concrete during and after the cooling phase of a fire, J. Fire Protect. Eng. 21 (2011) 245–263, https://doi.org/10.1177/1042391511423451.

[10] T. Gernay, Fire resistance and burnout resistance of reinforced concrete columns, Fire Saf. J. 104 (2019) 67–78, https://doi.org/10.1016/j.firesaf.2019.01.007.

[11] T. Molkens, The cooling phase, a key factor in the post-fire performance of RC columns, Fire Saf. J. 128 (2022) 103535, https://doi.org/10.1016/j.firesaf.2022.103535.

[12] V. Kodur, M. Dwaikat, R. Fike, High-temperature properties of steel for fire resistance modeling of structures, J. Mater. Civ. Eng. 22 (5) (2010) 423–434, https://doi.org/10.1061/(ASCE)MT.1943-5533.0000041.

[13] Y.C. Wang, Steel And Composite Structures: Behaviour And Design For Fire Safety", first ed., CRC Press, 2002 https://doi.org/10.1201/9781482267693.

[14] T. Gernay, Fire resistance and burnout resistance of timber columns, Fire Saf. J. 122 (2021) 103350, https://doi.org/10.1016/j.firesaf.2021.103350.

[15] F. Wiesner, A. Bartlett, S. Mohaine, F. Robert, R. McNamee, J.C. Mindeguia, L. Bisby, Structural capacity of one-way spanning large-scale Cross-Laminated Timber slabs in standard and natural fires, Fire Technol. 57 (2021) 291–311, https://doi.org/10.1007/s10694-020-01003-y.

[16] F. Wiesner, R. Hadden, S. Deemy, L. Bisby, Structural fire engineering considerations for cross-laminated timber walls, Construct. Build. Mater. 323 (2022) 126605, https://doi.org/10.1016/j.conbuildmat.2022.126605.

[17] Y. Katakura, H. Kinjo, T. Hirashima, S. Yusa, K. Saito, Deflection behaviour and load-bearing-period of structural glued laminated timber beams in fire including colling phase, in: Proceedings of the 9th International Conference on Structures in Fire (SiF), Princeton University, USA, 2016.

[18] T. Gernay, J. Zehfuß, S. Brunkhorst, F. Robert, P. Bamonte, R. McNamee, S. Mohaine, J.-M. Franssen, Experimental investigation of structural failure during the cooling phase of a fire: Timber columns, Fire Mater. (2022) 1–16, https://doi.org/10.1002/fam.3110.

[19] A. Lucherini, D. Šejnová Pitelková, V. Mozer, Predicting the effective char depth in timber elements exposed to natural fires, including the cooling phase, in: Proceedings of the World Conference on Timber Engineering (WCTE 2023), 2023. Oslo, Norway.

[20] European Committee for Standardization (CEN), EN 1995-1-2 Eurocode 5: Design of Timber Structures – Part 1.2, General – Structural fire design, Brussels, Belgium, 2004.

[21] S. Huc, R. Pecenko, T. Hozjan, Predicting the thickness of zero-strength layer in timber beam exposed to parametric fires, Eng. Struct. 229 (2021) 111608, https://doi.org/10.1016/j.engstruct.2020.111608.

[22] R. Emberley, A. Inghelbrecht, Z. Yu, J.L. Torero, Self-extinction of timber, Proc. Combust. Inst. 36 (2) (2017) 3055–3062, https://doi.org/10.1016/j.proci.2016.07.077.

[23] E. Annerel, L. Taerwe, B. Merci, D. Jansen, P. Bamonte, R. Felicetti, Thermo-mechanical analysis of an underground car park structure exposed to fire, Fire Saf. J. 57 (2013) 96–106, https://doi.org/10.1016/j.firesaf.2012.07.006.

[24] C. Abecassis-Empis, P. Reszka, T. Steinhaus, A. Cowlard, H. Biteau, S. Welch, G. Rein, J.L. Torero, Characterisation of Dalmarnock fire test one, Exp. Therm. Fluid Sci. 32 (2008) 1334–1343, https://doi.org/10.1016/j.expthermflusci.2007.11.006.

[25] P.H. Thomas, A.J.M. Heselden, Fully developed Fires in single compartments, in: CIB Report No. 20, Fire Research Note 923, Fire Research Station, London, 1972.

[26] M. Law, A Basis for the Design of fire Protection of building structures, Struct. Eng. 61A (1) (1983) 25–33.

[27] A.A. Khan, A. Usmani, J.L. Torero, Evolution of fire models for estimating structural fire-resistance, Fire Saf. J. 124 (2021) 103367, https://doi.org/10.1016/j.firesaf.2021.103367.

[28] J.F. Cadorin, J.M. Franssen, A tool to design steel elements submitted to compartment fires—OZone V2. Part 1: pre- and post-flashover compartment fire model, Fire Saf. J. 38 (5) (2003) 395–427, https://doi.org/10.1016/S0379-7112(03)00014-6.

[29] J.F. Cadorin, J.M. Franssen, A tool to design steel elements submitted to compartment fires – ozone V2. Part 2: Methodology and application, Fire Saf. J. 38 (5) (2003) 429–451, https://doi.org/10.1016/S0379-7112(03)00015-8.

[30] D. Peacock R.D. Richard, P.A. Reneke, G.P. Forney, "CFAST – consolidated model of fire growth and smoke transport (version 7). Volume 2: user's guide", NIST Technical Note 1889v2, National Institute of Standards and Technology (NIST) (2021) https://doi.org/10.6028/NIST.TN.1889v2.

[31] C. Wade, G. Baker, K. Frank, R. Harrison, M. Spearpoint, B-RISK user Guide and technical manual, in: SR364, Building Research Association of New Zealand, 2016.

[32] R. Hasib, R. Kumar, S. Kumar, Simulation of an experimental compartment fire by CFD, Build. Environ. 42 (9) (2007) 3149–3160, https://doi.org/10.1016/j.buildenv.2006.08.002.

[33] National Institute of Standards and Technology (NIST), Fire Dynamics Simulator (FDS), 2022. https://pages.nist.gov/fds-smv/.

[34] J.M. Franssen, T. Gernay, Modelling structures in fire with SAFIR(R): theoretical background and capabilities, J. Struct. Fire Eng. 8 (3) (2017) 300–323, https://doi.org/10.1108/JSFE-07-2016-0010.

[35] OpenFIRE. "OpenSEES for fire". http://openseesforfire.github.io/openfire.

[36] European Committee for Standardization (CEN), EN 1991-1-2 Eurocode 1: Actions On Structures – Part 1.2: General Actions – Actions On Structures Exposed to Fire, 2002. Brussels, Belgium.

[37] U. Wickström, Temperature calculation of insulated steel columns exposed to natural fire, Fire Saf. J. 4 (4) (1981) 219–225, https://doi.org/10.1016/0379-7112(81)90024-2.

[38] U. Wickström, Application of the standard fire curve for expressing natural fires for design purposes, Fire Safety: Science and Engineering (1985), https://doi.org/10.1520/STP35295S. ASTM International, STP35295S.

[39] S.E. Magnusson, S. Thelandersson, Temperature - time Curves of complete Process of fire development, in: Bulletin of Division of Structural Mechanics and Concrete Construction, vol. 16, Lund Institute of Technology, 1970.

[40] O. Pettersson, S.E. Magnusson, J. Thor, Fire engineering Design of steel structures, in: Bulletin of Division of Structural Mechanics and Concrete Construction, vol. 52, Lund Institute of Technology, 1976.

[41] D. Hopkin, R. Van Coile, C. Hopkin, K. LaMalva, M. Spearpoint, C. Wade, Design Fires and actions, International Handbook of Structural Fire Engineering, The Society of Fire Protection Engineers Series. LaMalva K (2022), https://doi.org/10.1007/978-3-030-77123-2. Hopkin D.

[42] R. Feasey, B. Buchanan, Post-flashover fires for structural design, Fire Saf. J. 37 (2002) 83–105, https://doi.org/10.1016/S0379-7112(01)00026-1.

[43] A. Lucherini, B. Jovanović, R. Van Coile, B. Merci, Background and limitations of the Eurocode parametric fire curves, including the fire decay phase, in: Proceedings of the 7th International Conference on Applications of Structural Fire Engineering, ASFE'21), Ljubljana, Slovenia, 2021.

[44] C.R. Barnett, BFD curve: a new empirical model for fire compartment temperatures, Fire Saf. J. 37 (5) (2002) 437–463, https://doi.org/10.1016/S0379-7112(02)00006-1.

[45] C.R. Barnett, G.C. Clifton, Examples of fire engineering design for steel members, using a standard curve versus a new parametric curve, Fire Mater. 28 (2004) 309–322, https://doi.org/10.1002/fam.860.

[46] C.R. Barnett, Replacing international temperature–time curves with BFD curve, Fire Saf. J. 42 (2007) 321–327, https://doi.org/10.1016/j.firesaf.2006.11.001.

[47] Deutsches Institut für Normung (DIN), DIN EN 1991-1-2/NA Eurocode 1: Actions on Structures – Part 1.2: General Actions – Actions on Structures Exposed to Fire, National Annex - Nationally determined parameters, Berlin, Germany, 2015.

[48] J. Zehfuss, D. Hosser, A parametric natural fire model for the structural fire design of multi-storey buildings, Fire Saf. J. 42 (2) (2007) 115–126, https://doi.org/10.1016/j.firesaf.2006.08.004.

[49] T.T. Lie, Characteristics temperature curves for various fire severities, Fire Technol. 10 (4) (1974) 315–326, https://doi.org/10.1007/BF02589990, 1974.

[50] J.R. Mehaffey, Performance-based Design of fire Resistance in wood-frame buildings, in: Proceedings of the 8th Interflam Conference, 1999. Egham, UK.

[51] Z. Ma, P. Makelainen, Parametric temperature-time curves of medium compartment fires for structural design, Fire Saf. J. 34 (4) (2000) 361–375, https://doi.org/10.1016/S0379-7112(00)00008-4.

[52] K. Hertz, Parametric fires for structural design, Fire Technol. 48 (2012) 807–882, https://doi.org/10.1007/s10694-011-0246-5.

[53] T. Lennon, D. Moore, The natural fire safety concept - full-scale tests at Cardington, Fire Saf. J. 38 (2003) 623–643, https://doi.org/10.1016/S0379-7112(03)00028-6.

[54] D. Drysdale, An Introduction to Fire Dynamics, third ed., John Wiley & Sons, 2011 https://doi.org/10.1002/9781119975465.ch1.

[55] S. Welch, A. Jowsey, S. Deeny, R. Morgan, J.L. Torero, BRE large compartment fire tests—Characterising post-flashover fires for model validation, Fire Saf. J. 42 (8) (2007) 548–567, https://doi.org/10.1016/j.firesaf.2007.04.002.

[56] A. Lucherini, J.L. Torero, Defining the fire decay and the cooling phase of post-flashover compartment fires, Fire Saf. J. 141 (2023) 103965, https://doi.org/10.1016/j.firesaf.2023.103965.

[57] J.L. Torero, A.H. Majdalani, C. Abecassis-Empis, A. Cowlard, Revisiting the compartment fire, Fire Saf. Sci. 11 (2014) 28–45, https://doi.org/10.3801/IAFSS.FSS.11-28.

[58] T.Z. Harmathy, A new Look at compartment fires, parts I and II, Fire Technol. 8 (3–4) (1972) 196–217, https://doi.org/10.4224/40001751, 326-351.

[59] B. Karlsson, J.G. Quintiere, Enclosure Fire Dynamics", first ed., CRC Press, 2000.

[60] V. Gupta, C. Maluk, J.L. Torero, J.P. Hidalgo, Analysis of convective heat Losses in a full-scale compartment fire experiment, Proceedings of the 9th International Seminar on Fire and Explosion Hazards (ISFEH9), Saint Petersburg, Russia (2019), https://doi.org/10.18720/spbpu/2/k19-53.

[61] I.R. Thomas, I.D. Bennetts, Fires in enclosures with single ventilation openings – comparison of long and wide enclosures, in: Fire Safety Science - Proceedings of the 6th International Symposium, 1999, pp. 941–952.

[62] J. Stern-Gottfried, G. Rein, L. Bisby, J.L. Torero, Experimental review of the homogeneous temperature assumption in post-flashover compartment fires, Fire Saf. J. 45 (2010) 249–261, https://doi.org/10.1016/j.firesaf.2010.03.007.

[63] V. Gupta, J.P. Hidalgo, D. Lange, A. Cowlard, C. Abecassis-Empis, J.L. Torero, A review and analysis of the thermal exposure in large compartment fire experiments, International Journal of High-Rise Buildings 10 (4) (2021) 345–364, https://doi.org/10.21022/IJHRB.2021.10.4.345.

[64] P.S. Veloo, J.G. Quintiere, Convective heat transfer coefficient in compartment fires, J. Fire Sci. 31 (5) (2013) 410–423, https://doi.org/10.1177/0734904113479001.

[65] T. Tanaka, A model of multiroom fire spread, Fire Sci. Technol. 3 (2) (1983) 105–121, https://doi.org/10.3210/fst.3.105.

[66] A. Jowsey, Fire imposed heat fluxes for structural analysis, School of Engineering, University of Edinburgh (2006). PhD thesis, http://hdl.handle.net/1842/1480.

[67] U. Wickström, D. Duthinh, K. McGrattan, Adiabatic surface temperature for calculating heat transfer to fire exposed structures, in: Proceedings of the 11th Interflam Conference, 2007. Egham, UK.

[68] C.H. Chen, J.S. T'Ien, Diffusion flame stabilization at the leading edge of a fuel plate, Combust. Sci. Technol. 50 (4–6) (1986) 283–306, https://doi.org/10.1080/00102208608923938.

[69] F.P. Incropera, D.P. DeWitt, T.L. Bergman, A.S. Lavine, Fundamental Of Heat and Mass Transfer, sixth ed., John Wiley & Sons, 2006.

[70] M. Luo, Effects of Radiation on temperature Measurement in a fire environment, J. Fire Sci. 15 (6) (1998) 443–461, https://doi.org/10.1177/073490419701500602.

[71] J. Francis, T.M. Yau, On radiant network models of thermocouple error in pre and post flashover compartment fires, Fire Technol. 40 (3) (2004) 277–294, https://doi.org/10.1023/b:fire.0000026974.18642.a1.

[72] J. Chlouba, F. Wald, Z. Sokol, Temperature of connections during fire on steel framed building, International Journal of Steel Structures 9 (2009) 47–55, https://doi.org/10.1007/BF03249479.

[73] M. Mensinger, P. Schaumann, M. Stadler, J. Sothmann, *Membranwirkung von Verbunddecken im Brandfall"*. Faculty of Civil Engineering and Geodesy, Chair for Metal Structures, Technical University of Munich, 2011, https://doi.org/10.13140/2.1.1164.9286.

[74] A. Nadjai, C.G. Bailey, O. Vassart, S. Han, B. Zhao, M. Hawes, J.M. Franssen, I. Simms, Full-scale fire test on a composite floor slab incorporating long span cellular steel beams, Struct. Eng. 89 (21) (2011) 18–25.

[75] F. Wald, T. Jána, K. Horová, Design of joints to composite columns for improved fire robustness, To Demonstration fire tests (2011). Czech Technical University in Prague, ISBN 978-80-01-04871-9, http://fire.fsv.cvut.cz/test-veseli-2011/.

[76] A. Lucherini, Fundamentals of thin intumescent coatings for the design of fire-safe structures, School of Civil Engineering, The University of Queensland (2020), https://doi.org/10.14264/uql.2020.1021. PhD thesis.

[77] A. Bejan, Convection Heat Transfer", fourth ed., John Wiley & Sons, 2013.